

ISSN 0038-0806

# SOILS and FOUNDATIONS

Vol.23, No.4  
Dec. 1983



The Japanese Society of Soil Mechanics  
and Foundation Engineering

## EFFECT OF STATIC SHEAR ON RESISTANCE TO LIQUEFACTION\*

Discussion by RAMLI MOHAMAD\*\* and RICARDO DOBRY\*\*\*

The authors have contributed very significantly towards clarifying the effect of an initial static shear stress on cyclic liquefaction resistance by recognizing and investigating separately the influence of the following:

- (i) Relative density,
- (ii) Reversal or non-reversal of shear stresses.

Relative density is shown to be crucial in the way it determines whether flow deformation is possible, i.e., whether the sand is contractive. Reversal or non-reversal of shear stresses is shown to be important in the way it "decides" whether transient or initial liquefaction can occur, and hence, the way it influences the rate of strain accumulation.

The authors do all their triaxial tests at an effective minor consolidation stress  $\sigma_{3c}' = 2.0 \text{ kgf/cm}^2$ . The writers believe that a more general and systematic analysis of the effect of initial shear would be possible if the influence of both relative density and minor consolidation stress are considered together. By doing so, and by combining with steady state concepts as developed and described by Castro (1969, 1975), Castro and Poulos (1977), Poulos (1981), Casagrande (1976) and Castro et al. (1982), much light can be shed on the problem.

The  $e$  vs  $\log \sigma_3'$  steady state line (SSL) or  $e_f$ -line for a batch of Banding Sand (Sand B), modified from Castro (1969) is shown in Fig. 14(a) (The writers have modified the plot from Castro's original figure by fitting

a straight line, for simplicity). Specimens with initial states (at the end of consolidation) which are significantly to the right of the  $e$  vs  $\log \sigma_3'$  SSL are *contractive* while those with initial states to the left of this SSL are *dilatative*. Specimens consolidated to a state slightly to the right of the SSL are *partially-contractive*. In reality there is some

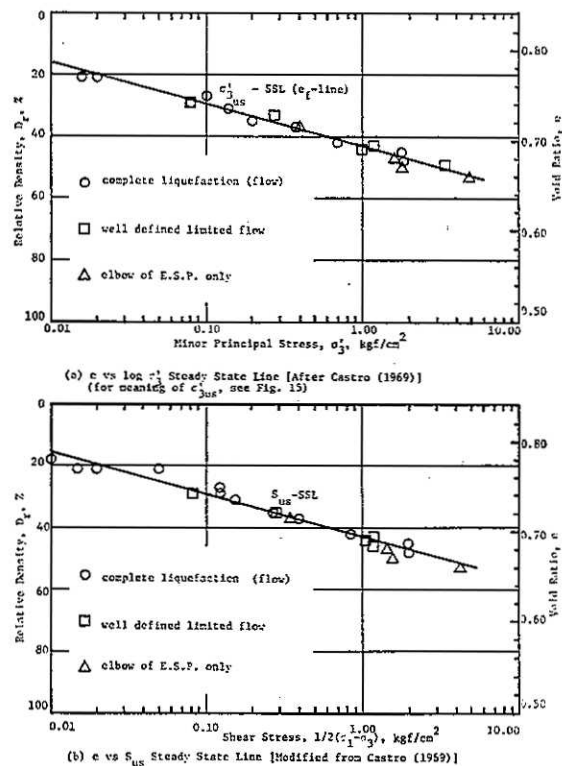


**Fig. 14. State diagrams for banding sand (sand B)**

\* By Y. P. Vaid and J. C. Chern, Vol. 23, No. 1, March 1983, pp. 47-60.

\*\* Graduate Student, Dept. of Civil Engineering, Rensselaer Polytechnic Institute, Troy, NY, USA.

\*\*\* Professor, Dept. of Civil Engineering, Rensselaer Polytechnic Institute, Troy, NY, USA.

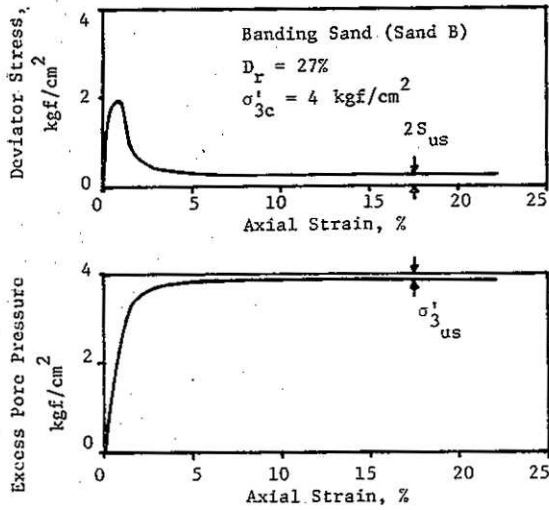


Fig. 15. Typical stress-strain-pore pressure response of a contractive sand specimen in CIU-test (After Castro, 1969)

overlap among the various zones.

Contractive specimens are susceptible to flow deformation, and a typical stress-strain curve from a monotonic load-controlled CIU-test is shown in Fig. 15. Castro and his co-workers have shown that the effective stresses during flow deformation are functions of only the void ratio (or relative density) of a sand. Castro et al. (1982) have thus shown that it is also possible to plot the steady state shear strength during flow (or residual shear strength), defined as  $S_{us} = 1/2(\sigma_1 - \sigma_3)_{us}$ , versus relative density (the subscript "us" denotes "undrained steady state"). Such a plot, constructed by the writers based on Castro's (1969) data for the same Banding Sand of Fig. 14(a), is shown in Fig. 14(b).

Based on plots such as in Fig. 14, it is now possible to systematically interpret the effects of initial shear on cyclic liquefaction resistance measured in cyclic triaxial tests as follows.

*Contractive Specimens*

An effective stress path for a stress-controlled cyclic triaxial test on an anisotropically consolidated, contractive specimen is re-

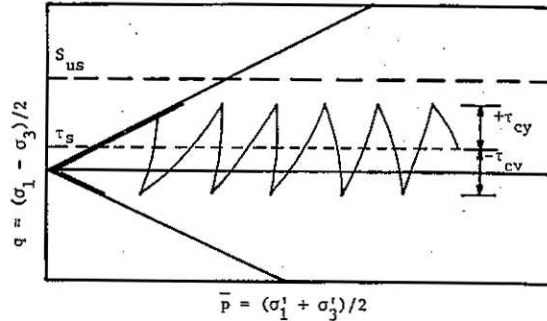


Fig. 16. Schematic effective stress path showing effect of increasing initial shear on behavior of contractive sand specimen in cyclic, stress controlled, undrained triaxial test

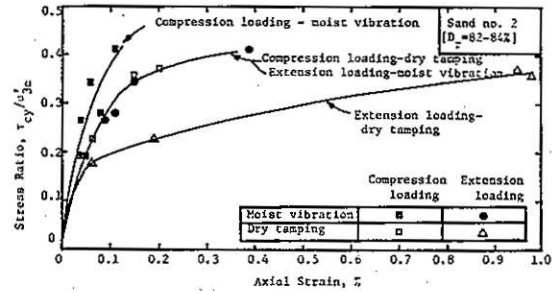


Fig. 17. Stress-strain curves for first compression and extension excursions, stress-controlled cyclic triaxial tests, sand No. 2 (Dobry et al, 1982; Modified after Iadd, 1977)

presented schematically in Fig. 16. The magnitude of the steady state shear strength,  $S_{us}$ , corresponding to the void ratio of the specimen is also shown. For convenience, let the magnitude of the cyclic shear stress,  $\tau_{cy} = 1/2 \sigma_{dcy}$ , be fixed, with a value less than  $S_{us}$ . The peak shear stress is thus given by  $\tau_p = \tau_s + \tau_{cy}$ . Castro et al. have shown that if  $\tau_p$  is less than  $S_{us}$ , continuous, unidirectional, flow deformation can never occur. Also, in the case of reversing shear stresses, there is evidence that the larger the extension-reversal component, the larger are both the strain and pore pressure buildup (Dobry et al., 1982). Fig. 17 shows clearly the effect on strain, and the difference is seen to be larger at higher values of cyclic stress, and to depend on the method of sample preparation. Although the results shown in

Fig. 17 are for the first cycle of tests performed on isotropically consolidated dense specimens, they serve to indicate the severity of the effects of shear stress reversal on the value of the strain and thus also on the pore pressures. Similar evidence on the influence of stress reversal for looser sands, in anisotropically consolidated cyclic triaxial tests, has been provided by Lee and Seed (1967). Therefore, in contractive specimens tested with the same  $\tau_{cy}$ , the increase of  $\tau_s$  corresponds to a decrease in degree of reversal, and for  $\tau_p < S_{us}$ , this should *always* result in lower strains and pore pressures, and thus in an increased liquefaction resistance.

With reversing shear stresses of a given magnitude,  $\tau_{cy}$ , increasing  $\tau_s$  can result in either or both of two events: elimination of stress reversal, and/or the condition  $\tau_p > S_{us}$ . The results of extensive tests by Castro et al have shown that with non-reversing shear stresses *and*  $\tau_p > S_{us}$ , the liquefaction resistance always decreases as  $\tau_s$  increases. Thus, as  $\tau_s$  or  $K_c$  is consistently increased, there should be a turning point from increasing resistance (due to decreasing reversal component) to decreasing resistance (due to  $\tau_p > S_{us}$  and removal of stress reversal). Therefore, the conditions of (i)  $\tau_p > S_{us}$ , and (ii) elimination of shear stress reversal, should define bounds for this turning point in resistance. If the value of  $S_{us}$  is known,

these bounds can be determined. This is done in what follows for the results presented by the authors.

First, it is found more convenient to recast the authors' plot in Fig. 12 in the form:  $\tau_{cy}/\sigma_{3c}'$  vs  $K_c$ , as shown in Fig. 18 for  $D_r = 45\%$ .

For the condition of  $\tau_p$  exceeding  $S_{us}$ :

$$\tau_p = \tau_s + \tau_{cy} > S_{us} \quad (2)$$

A bound is

$$\tau_s + \tau_{cy} = S_{us} \quad (3)$$

Substituting

$$\tau_s = \frac{1}{2}(\sigma_{1c}' - \sigma_{3c}') \quad (4a)$$

and

$$K_c = \sigma_{1c}'/\sigma_{3c}' \quad (4b)$$

into (3) gives

$$\tau_{cy}/\sigma_{3c}' = -\frac{1}{2}K_c + \left(\frac{1}{2} + S_{us}/\sigma_{3c}'\right) \quad (5)$$

From Fig. 8, the value of  $S_{us} \approx 0.32 \text{ kgf/cm}^2$  is obtained for the Ottawa sand with  $D_r = 45.9\%$ , which is practically the same as that corresponding to Fig. 18. Substituting this value and  $\sigma_{3c}' = 2.00 \text{ kgf/cm}^2$  into Eq. (5) gives a straight line defining one of the above bounds of turning points in resistance. This line is plotted in Fig. 18.

The other bound of the turning point is the line separating the region of stress reversal from that of no stress reversal. This line is given by

$$\frac{\tau_{cy}}{\sigma_{3c}'} = \frac{1}{2}(K_c - 1) \quad (6)$$

This line is also shown in Fig. 18. Since this line given by Eq. (6) lies to the right of that given by Eq. (5), the condition of  $\tau_p > S_{us}$  is also satisfied in the region of no stress reversal. It is predicted that in zone A, where there is shear stress reversal *and*  $\tau_p < S_{us}$ , the cyclic resistance *always* increases with increasing  $\tau_s$  and  $K_c$ . In zone C, where there is no reversal *and*  $\tau_p > S_{us}$ , it is predicted that increasing  $\tau_s$  and  $K_c$  *always* decreases the cyclic resistance. Thus, in Zone B (shaded), which lies in between, there should be a turning point in resistance. All of the above predictions are fully validated

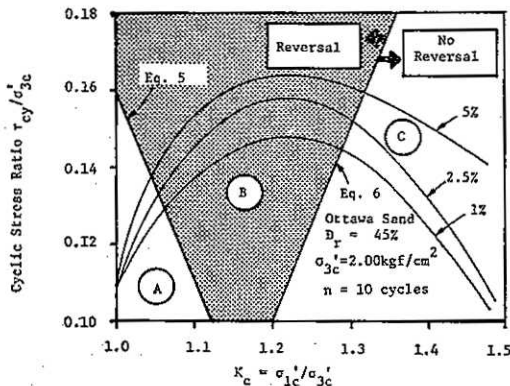


Fig. 18. Cyclic stress ratio required to cause specified accumulated axial strain in 10 stress cycles for loose Ottawa-Sand (Modified from author's data)

by Fig. 18, which is based on the authors' results.

In Fig. 18, it can also be seen that for the Ottawa Sand, and with the sample preparation technique used by the authors, decreasing the extension-reversal branch in Zone B has a stronger influence on the resistance than  $\tau_p$  exceeding  $S_{us}$ , since all the turning points in the curve are to the right of the line of symmetry of the zone, given by  $K_c=1.16$ .

#### *Dilative Specimens*

Similar arguments can be applied to dilative specimens, also reported by the authors, but with the following very important difference. Because a dilative specimen cannot flow, there is no  $S_{us}$ , and a line given by Eq. (5) does not exist. Therefore, all factors associated with increasing  $\tau_s$  and  $K_c$  now tend to increase the liquefaction resistance, and no decreasing branch of the curve such as shown in Fig. 18 should exist. This, of course, is what the authors found for their tests on dense sand with  $D_r=65\%$ . Also, in contrast to contractive behavior, the response of a dilative sand when the effective stress path meets the strength envelope is to tend to slow down or to stop strain buildup by virtue of its dilative tendency. Youd (1973) describes this stage as "solidification." Additional cyclic stresses induce very small strains, and hence strain accumulation is also stabilized. Strains mostly accumulate prior to reaching the strength envelope. This trend can be observed in the tests by Castro et al. (1982). Thus, for dilative specimens, the larger the value of  $\tau_s$ , the shorter is the horizontal distance which the effective stress path has to traverse in order to reach the strength envelope, and the less opportunity there is for strain accumulation. This also contributes to increasing the resistance of the specimen with increasing  $\tau_s$ .

#### *Partially-Contractive Specimens*

Partially contractive specimens are defined here as those which exhibit a limited flow stage followed by a dilative stage under un-

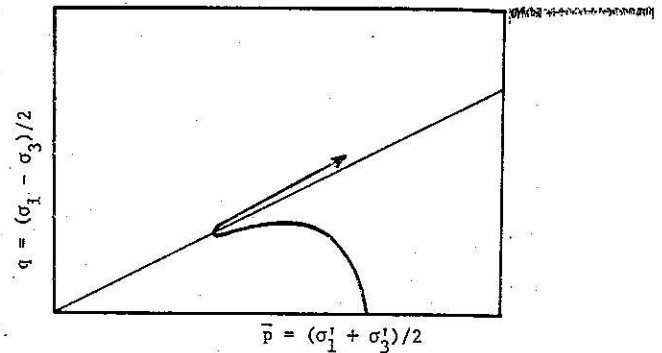


Fig. 19. Schematic effective stress path for partially-contractive sand specimen in CIU-test

drained monotonic loading. This behavior is characterized by an effective stress path as shown schematically in Fig. 19. The limited flow stage takes place at the point where the effective stress path bends sharply to the right, which the writers call the "elbow." Again, using Castro's (1969) raw data, the writer has plotted the values of  $q=1/2(\sigma_1-\sigma_3)$  corresponding to such "elbow" points for Sand B in Fig. 14(b). It can be seen that the shear stress at the "elbow" is practically the same residual  $S_{us}$  obtained from tests with complete flow failure.

The effect of an initial shear stress on a partially contractive specimen would thus be similar to that of a contractive specimen at small specified failure strain levels, and similar to that of a dilative specimen at large specified strain levels.

From Fig. 8, it is clear that the monotonic stress-strain curve S-2 for the Ottawa Sand with  $D_r=45.9\%$ , is not purely contractive. However, Fig. 12 and Fig. 18 suggest that the sample is still exhibiting contractive behavior at a specified strain level of 5%, while the monotonic test shows that dilative response begins at about 3% axial strain. The reason for this difference is believed to be the following: Fig. 12 uses the accumulated strains, i. e., the sum of permanent and cyclic strains, whereas in Fig. 8 the strain is due to a single load application. Therefore, the contractive behavior in Fig. 12 may perhaps be due to the cyclic component of the

accumulated strain, which is still less than the 3% required to make the specimen dilative.

#### References

- 21) Castro, G. and Poulos, S. J. (1977) : "Factors affecting liquefaction and cyclic mobility," Journal of the Geotechnical Engineering Division, ASCE, Vol. 103, GT 6, pp. 501-516.
- 22) Castro, G., Poulos, S. J., France, J. W. and Enos, J. L. (1982) : "Liquefaction induced by cyclic loading," Geotechnical Engineers, Inc. -Report Submitted to National Science Foundation.
- 23) Dobry, R., Ladd, R. S., Yokel, F. Y., Chung, R. M. and Powell, D. (1982) : "Prediction of pore water pressure buildup and liquefaction of sands during earthquakes," National Bureau of Standards, Building Science Series 138, U. S. Dept. of Commerce.
- 24) Ladd, R. S. (1977) : "Specimen preparation and cyclic stability of sands," Journal of the Geotechnical Engineering Division, ASCE, Vol. 103, pp. 535-547.
- 25) Poulos, S. J. (1981) : "The steady state of deformation," Journal of the Geotechnical Engineering Division, ASCE, Vol. 107, GT 5, pp. 553-562.
- 26) Youd, T. L. (1973) : "Liquefaction, flow and associated ground failure," Circular 688, United States Geological Survey.